First CMS Results

Valerie Halyo for the CMS Collaboration

Department of Physics, Princeton University, Princeton, NJ 08544, USA

DOI: http://dx.doi.org/10.3204/DESY-PROC-2010-01/267

Already in 2006 with 25M muons accumulated during the Magnet Test and Cosmic Challenge with only a small fraction of the sub detector installed on the surface, CMS worked towards its first measurement of charge asymmetry of atmospheric muons that was published [8] once combined with the 270M muons accumulated during Cosmic Run at four Tesla (CRAFT) in 2008. This result was followed by the first CMS measurements of $\mathrm{dN/d}\eta$ $\mathrm{dN/d}p_T$ [3], the underlying event activity [5], two particle correlation [6], Bose-Einstein Correlations (BEC) [7], and the observation of diffractive events [4] presented in the talk. These first measurements were based on collision data taken during the successful startup at 2009 where LHC delivered about 15 μb^{-1}/ 1 μb^{-1}at collision energy of 0.9 TeV /2.36 TeV correspondingly and followed at 2010 with the first proton-proton collisions at center of mass energy at 7 TeV.

1 Introduction

The CMS experiment collected approximately 350 thousand collision events at an energy of $\sqrt{s} = 0.9$ TeV and 20 thousand events at $\sqrt{s} = 2.36$ TeV with good detector conditions and the magnet switched on at the nominal value of 3.8T. This corresponds to about 10 $\mu b^{-1}$of integrated luminosity and 0.4 μb^{-1}correspondingly. In 2010 CMS recorded the first proton proton collision at 7TeV delivered by LHC. At the time of the presentation CMS recorded about 20 n$b^{-1}$and in the eight weeks to follow LHC will deliver another 3.6 pb^{-1}. The recorded data sample is smaller than needed to do the physics studies for which CMS was designed. However, it is sufficient to assess the general quality and the proper functioning of the detector, the algorithms modeling of the detector response in the simulation and the properties of the inelastic events based on the first CMS measurement which are the primary focus of my presentation. These first measurements can be categorized into two classes consisting the primary ingredients necessary to understand inelastic collisions before proceeding to do higher level measurements. The first class of measurements [3]-[5] shed light on the understanding of the single particle properties that is essential to understand the mechanism for hadron production and the relative role of soft and hard contribution at the highest collision energy. The basic properties of charged tracks such as charged hadron multiplicities vs transverse momentum or pseudorapidity, the study of the underlying event activity and the observation diffractive process were presented. These measurements are also base line for HI physics and future measurements with pile up. The second class of measurements [6]-[7] done by CMS provides higher understanding of the correlations between the single particles leading to two studies, the two particle correlation and BEC. These measurements are also base line for Heavy Ion (HI) physics where the correlation will depend on the centrality of the event. These two fundamental categories are essential for

conforming that we understand our detector and improve our current understanding of the inelastic processes. Section 2 briefly presents the performance of the tracker, which is most relevant for the first measurements. Section 3 describes the common selection criteria for these measurements and subsection 4.1-4.5 presents briefly each of the first results presented in the talk. Section 5 draws the conclusions from the first CMS measurements [3]-[7] and summarize CMS near future plans.

2 CMS Tracker Performance

Excellent performance of the CMS silicon tracker and tracking algorithms [1] was a crucial ingredient for the first CMS measurements. Both the resolution of the primary vertices and the use of the dE/dx for particle identification were essential for the first CMS measurements and were described briefly in the talk. Beam spot and primary vertices are reconstructed with high efficiency and resolution close to the expectation from simulation. The primary vertex resolution was found to depend strongly on the number of tracks used in fitting of the vertex and the pT of those tracks. This results indicated that for momentum range and number of tracks used in these measurement we were able to reach a primary vertex resolution of about 100 μm with only few tracks, helping us to efficiently select the events. The other advantage provided by the tracker is the excellent particle identification with dE/dx used by BEC measurement [7]. Figure 1 shows the distribution of dE/dx versus momentum for particle-calibrated data. The bands departing toward high dE/dx values at low momentum are attributed to kaon, proton and deuteron tracks, respectively. The fit to the proton band restricted to the range [0.7, 1.0] GeV/c is shown as a red curve in Fig. 1, while the black curves show agreement with the fit results extracted from the proton fit results. The mass spectrum resulting by inverting the dEdx equation used the dE/dx data for tracks with dE/dx $>$ 4.15 MeV/cm and p $<$ 2 GeV/c is shown in Fig. 2. The known values of the kaon and proton masses are also indicated as vertical lines on the plot. We observe an additional peak in data which is not visible in simulation, and we attribute it to deuterons This essential particle identification tool was already prooven to be useful in one of the first measurements and is planned to be used as one of the main handles for the search for new charged long-lived particles.

3 Event Selection Common to First Measurements

Common Min Bias event selection criteria were used in most of the first CMS measurements [3]-[7]. Online, events were selected by a trigger signal in any of the Beam Scintillator Counters (BSC) scintillators, coinciding with a signal from either of the two Beam Pickups Timing eXperiment (BPTX) detectors indicating the presence of at least one proton bunch crossing the IP. From these samples, collision events were selected offline by requiring BPTX signals from both beams passing the IP, Forward Hadronic (HF) Calorimeter energy larger than 3GeV on both sides of the HF (HF $2.9 < |\eta| < 5.2$) and an analysis dependent collision vertex requirement. In addition, beam-halo muons events identified by requiring the time difference between any two hits from the BSC stations on opposite sides of the IP to be within 73 ± 20 ns were removed from the data sample. Last but not least dedicate beam background events such beam-scraping/gas events were removed from the data sample.

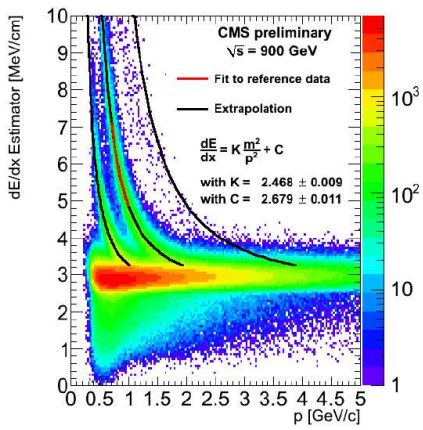

Figure 1: dE/dx versus p in data collected at 900 GeV during December 2009. red line: fit with proton mass assumption, in a restricted p range; black lines:extrapolations.

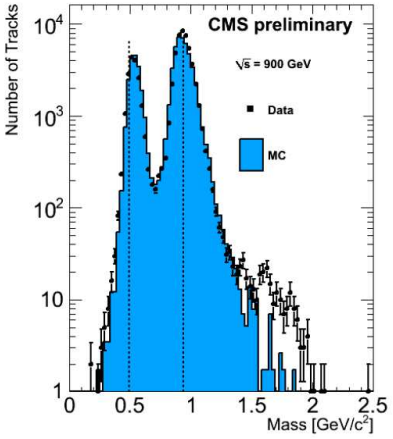

Figure 2: Mass distribution, using tracks with p < 2 GeV/c and dE/dx > 4.15 MeV/cm for 900 GeV data (dots with error bars) and simulation (solid).

4 First CMS Results

In the following a brief description of each of the first CMS results will be presented starting with the first class of measurements that aims to shed light on the understanding of the single particle properties essential to understand the mechanism for hadron production and the relative role of soft and hard contribution at the highest collision energy. The measurements belonging to this category are the transverse-momentum and pseudo-rapidity distributions of charged Hadrons at 7TeV [3], the Underlying Event Activity at 0.9TeV [5] and the observation of diffraction at 0.9TeV and 2.36TGeV [4]. The second class of measurements described in the following provides better understanding of the correlations between the single particles. The measurements in this class are the two particle correlation [6] and BEC [7].

4.1 Transverse-Momentum and Pseudorapidity Distributions of Charged Hadrons

Good understanding of the tracker performance allowed a timely publication of the first physics measurement from the first collisions data at 0.9TeV and 2.36TeV in 2009 [2] followed up with results at 7TeV from 2010 [3] collision data. In my talk I presented the measurement of the inclusive charged-hadron transverse-momentum and pseudo-rapidity distributions in proton-proton collisions at $\sqrt{s} = 7$TeV, which is the highest collision energy achieved at a particle collider to date. Measurements of $dN_{\rm ch}/dp_T$ and $dN_{\rm ch}/d\eta$ distributions and their $\sqrt{s}$ dependence are important for understanding the mechanisms of hadron production and the relative roles of soft and hard scattering contributions in the LHC energy regime. Three different methods with different sensitivity to potential systematic effects were combined in this measurement: pixel cluster counting, pixel tracklets, and full track reconstruction. The cluster counting method

correlates the observed pixel-cluster length in the z direction, expressed in number of pixels, with the expected path length traveled by a primary particle at a given η value. Background due to loopers, secondary particles and daughters of long-lived hadrons was removed. The pixel tracklets are constructed from combinations of two pixel hits in any two pixel barrel layers. The contribution from secondary particles, reconstruction efficiency and geometrical acceptance was evaluated using the PYTHIA simulations. The third method used both the pixel and the silicon strip tracker (SST) detectors to reconstruct tracks, including both barrel and endcap layers. The acceptance was limited to $|\eta| < 2.4$ to avoid edge effects. The measured yield in data was corrected, based on MC simulation and comparisons with data, for geometrical acceptance (2% correction for pT $>$ 200 MeV/c), efficiency of the reconstruction algorithm (5$-$10% for pT $>$ 300 MeV/c), fake and duplicate tracks ($<$ 1% each). The contamination of less than 2% from decay products of long-lived hadrons, photon conversions and inelastic hadronic interactions with the detector material was also subtracted. To obtain the $dN_{\rm ch}/d\eta$ result from the $p_{\rm T}$ spectrum, an extrapolation to pT = 0 was necessary, resulting in an increase of 5% in the estimated number of charged hadrons. Tracks with $|\eta| < 2.4$ and $p_T > 0.1$ GeV/c were used for the measurement of $1/(2\pi p_T) d^2N_{\rm ch}/d\eta dp_T$ as shown in Fig. 3

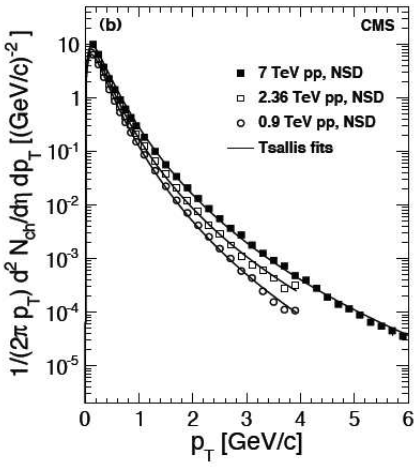

Figure 3: Measured yield of charged hadrons for $|\eta| < 2.4$ with systematic uncertainties (symbols) at 0.9, 2.36 and 7 TeV collision energy, fit with the empirical Tsallis function

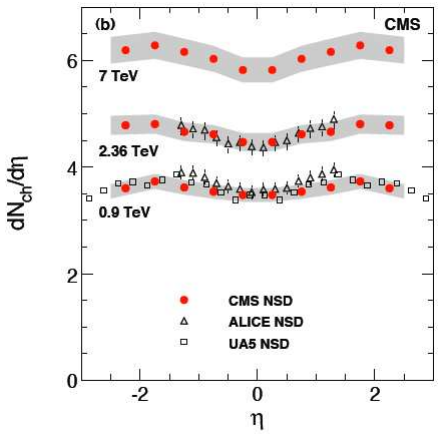

Figure 4: Reconstructed $dN_{\rm ch}/d\eta$distributions averaged over the cluster counting, tracklet and tracking methods, compared to data from the UA5 [10] (open squares) and from the ALICE [9] (opentriangles) experiments at 0.9 TeV.

The yield of charged-hadron in non-single-diffractive (NSD) events as a function of p_T was fitted by the Tsallis function which empirically describes both the low-pT exponential behavior corresponding to the beam beam remnant and the high-pT power-law behavior corresponding to the hard parton-parton collision. For the 7 TeV data, the average transverse momentum, calculated from the measured data points adding the low - and high-pT extrapolations from the fit is $\langle p_{\rm T} \rangle = 0.545 \pm 0.005$ (stat.) $\pm$ 0.015 (syst.) GeV/c. GeV/c. In addition, the measured yield

of charged hadrons at different collision energy as seen in Fig. 3 shows that the p_T spectrum gets harder at higher collision energy which is consistent with the increasing hadronic activity. The $dN_{\rm ch}/d\eta$ distribution was calculated as the weighted average of the data from the three reconstruction methods, taking into account their systematic uncertainties, and symmetrized in pseudorapidity. The averaged result is shown in Fig. 4 and is compared to measurements at the same accelerator (ALICE, [9]) and to previous measurements at the same energy but with different colliding particles (UA5, [10]). The shaded error band on the CMS data and the error bars for the data from ALICE indicates systematic uncertainties, while the error bars on the data from UA5 display statistical uncertainties only. No significant difference is observed between the $dN_{\rm ch}/d\eta$ distributions measured in pp and $p\overline{p}$ collisions at $\sqrt{s} = 0.9$ TeV. The $dN_{\rm ch}/d\eta$ distribution is found weakly eta-dependent, with a slow increase towards higher η values, and an indication of a decrease at $|\eta| > 2$. In the central region $|\eta| < 0.5$, the pseudorapidity density, $dN_{\rm ch}/d\eta$, has been measured to be 5.78 ± 0.01(stat.) $\pm$ 0.23(syst.) for non-single-diffractive events, higher than predicted by commonly used models. The relative increase in charged-particle multiplicity from $\sqrt{s} = 0.9$ to 7 TeV is 66.1% +/- 1.0% (stat) +/- 4.2% (syst). With the new measurement [3] at 7 TeV the study of particle production in pp collisions has been extended into a new energy regime.

4.2 Observation of diffraction in proton-proton collisions at 0.9 and 2.36TeV centre-of-mass energies

One of the systematics uncertainties in the measurement of inclusive charged-hadron transverse-momentum and pseudorapidity distributions for non-single-diffractive interactions [3] is the fraction of single diffractive to non diffractive events. Hence observation of single diffractive events is essential to properly describe these events in simulations. First observation of diffractive signal [4] dominated by the inclusive single diffractive (SD) reaction $pp \rightarrow Xp$ was based on 10 $\mu b^{-1}$of data collected at 0.9TeV and 0.4 μb^{-1}at 2.36TeV. Diffractive events can be described in terms of a colorless exchange with the vacuum quantum numbers (the "pomeron") and notably no color. Despite the substantial progress in the understanding of hard-diffractive events, in which a hard scale is present, in the framework of QCD (see e.g. [11]). the quantitative description of soft-diffraction still largely relies on Regge theory. The observed energy dependence of the inclusive single-diffractive cross section is however weaker than that expected by Regge theory, leading to an effect that is sometimes quantified in terms of the "rapidity gap survival probability". The acceptance of SD is high at LHC. The selection efficiency for SD events however, is model dependent and yields in about 20% according to PYTHIA and about 35% according to PHOJET; for non-diffractive (ND) events it is about 85% for both generators. In Fig. 5 we can find the distribution of the events as a function of $E \pm p_z = \sum i(E_i p_{z,i})$, where the sum runs over all calorimeter towers ($\eta < 5$). This variable would be proportional to the fractional energy loss of the scattered proton if the direction of the proton emitting the pomeron was known. The distributions are uncorrected. The bands illustrate the effect of a 10% energy scale uncertainty in the calorimeters and should be taken as a rough estimate of the systematic uncertainty due to the current imperfect understanding and simulation of the detector. At both energies, a clear diffractive contribution is evident. The data are compared with the predictions of PYTHIA (tune D6T) and PHOJET. The agreement is reasonable, with PYTHIA describing the ND part of the data better than PHOJET. To enhance the diffractive component in the data, a cut was applied to the HF energy sum. As an example, Fig. 5 shows the $E + p_z$, distributions for events in which the energy sum in HF- was $E_{HF-} < 8$ GeV (900

GeV data). This cut mainly selects single-diffractive events with a large rapidity gap (LRG) over HF- The system X is thus boosted towards the positive z direction. The data comparison to PYTHIA6 and PHOJET shows again that PYTHIA6 gives a better description of the non-diffractive component of the data, while PHOJET reproduces the diffractive contribution more accurately,

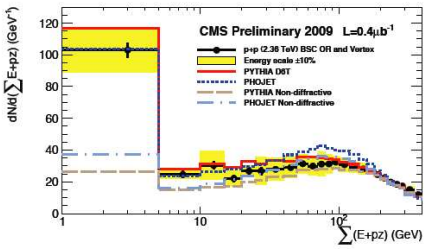

Figure 5: Distributions of the accepted events as a function of $E + pz$, 2360 GeV. The predictions of PYTHIA and PHOJET are also shown, normalised to the data. The distributions are uncorrected. The vertical bars indicate the statistical uncertainty of the data. The bands illustrate the effect of a 10% energy scale uncertainty in the calorimeters..

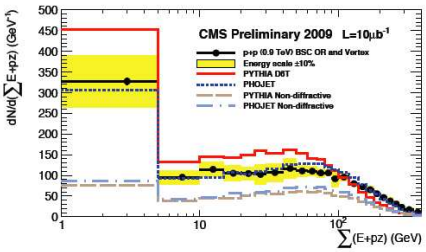

Figure 6: Distributions of $E + pz$ after the requirement of $E_{HF-} < 8$ GeV for the 900 GeV data. The distributions are uncorrected. The vertical bars indicate the statistical uncertainty of the data. The bands illustrate the effect of a 10% energy scale uncertainty in the calorimeters. The data are compared to both PYTHIA and PHOJET, normalised to the data

4.3 The Underlying Event Activity in Proton-Proton Collisions at 900 GeV

In parallel to the observation [4] of diffractive events dominated by the inclusive single diffractive CMS studied the underlying event activity [5] based on collision data at 900GeV. In the presence of a hard process the hadronic final states of hadron-hadron interactions can be described as the superposition of several contributions: products of the 2-to-2 hard parton scattering, including initial and final state radiation; hadron production in additional "multiple parton interactions"(MPI); and "beam-beam remnants" (BBR), resulting from the hadronization of the beam partonic constituents which did not participate in the hard scatter. Products of the MPI processes, which are mostly "soft", and BBR form the "underlying event" (UE). A good description of UE properties is crucial for precision measurements of Standard Model processes and for the search of physics beyond the Standard Model at the Large Hadron Collider(LHC) [12]. Predictions of several QCD models, after full detector simulation, were compared to the uncorrected data. Three distinct topological regions in the hadronic final state are thus defined in the plane transverse to the beam direction, using the angle difference, $\Delta\phi$, between the direction of the leading object and that of any charged hadron in the event. Hadron production in the "toward" region with $|\Delta\phi| < 60$ and in the "away" region with $|\Delta\phi| > 120$ is expected to be dominated by the hard parton-parton scattering and radiation. In contrast, the UE structure can be best studied in the "transverse" region with $60 < |\Delta\phi| < 120$. The analyses are performed by selecting events with a minimum value of the p_T of the leading object, which is either

a track or a track jet with $|\eta| < 2$. Requiring $p_T > 1$ GeV/c gets rid of most of the diffractive component of the collision, which sets the minimal scale for the studies. In Fig. 7 we find the average multiplicity per unit pseudorapidity for all tracks with $p_T > 0.5$ GeV. Here, the track selection is extended to $|\eta| = 2.5$. The multiplicities of particles with $p_T > 0.5$ GeV/c increase significantly with the scale fixed by the leading jet p_T. The various PYTHIA tunes describe within 10 % - 15% the overall features of the data: normalisation, η dependence and effect of the p_T cut on the leading jet. However, no description is really good, neither in normalization nor in shape. For both jet p_T cuts, the data show a significantly stronger η dependence than predicted by the PYTHIA models, although the shape description is slightly better with tunes P0 and Pro-Q20. Tune CW is too high in normalization, whereas tunes D6T, P0 and ProQ20 are generally too low, with DW being too low in the central region and too high at large $|\eta|$ values. The fact that the models underestimate activity at the lower scale it is not a surprise as the contamination from diffraction events is not well accounted in pythia. The CW tune was the last quick attempt to adjust the MPI level but overshot by a bit suggesting the correct tune is within reach.

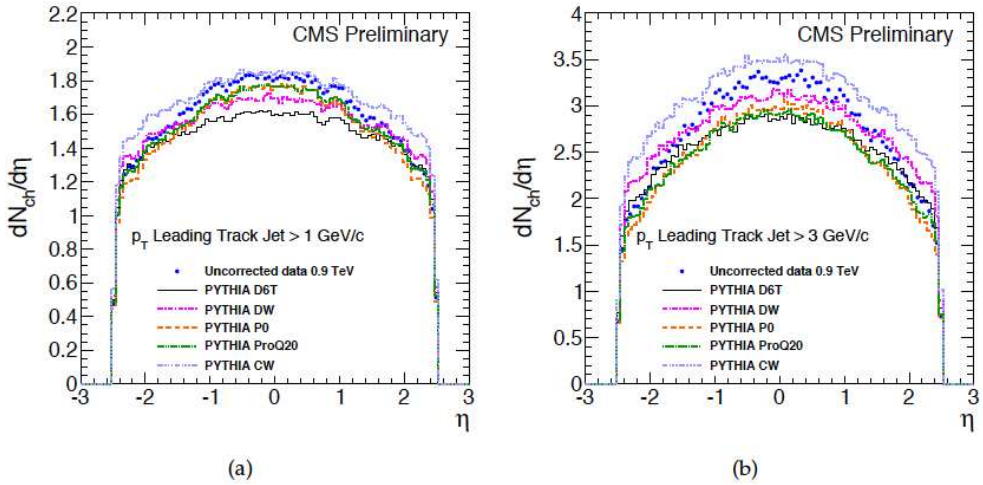

Figure 7: Average multiplicity, per unit of pseudorapidity, of charged particles with $pT > 0.5$ GeV/c, as a function of η. The leading track jet is required to have $|\eta| < 2$ and (a) $pT > 1$ GeV/c; (b) > 3 GeV/c (note the different vertical scales). Predictions from several PYTHIA MC tunes are compared to the uncorrected data.

In Fig. 8 one finds the charged particle density in transverse region versus event p_T scale. The turn on curve is correlated with the centrality of the collision, reaching head on collision at 4 GeV. The slow increase in multiplicity is related to the increase in MPI. Once again one finds that DW and CW predictions embrace the data. Similar results were seen for the multiplicity of charged particles, the sum p_T distribution and the p_T distribution of charged hadrons in the the transverse region. To summarize we find that for the 900 GeV the predictions were about 10% lower than expected however they can be tuned easily to agree with the 900GeV , 7TeV and Tevatron collision data. (see X1(Rick Field, TuneAMBT1 from Atlas.). In addition, the measurements exhibit a preference for higher values of the energy dependence, i.e. $\epsilon = 0.25$

(as in tune DW) or 0.30 (as in tune CW) and over $\epsilon = 0.16$ (original Atlas tune). Lower values of 0.16 as in tune D6T are disfavored. The analysis on 7 TeV data as well as corrections for detector effects are ongoing while in parallel an investigation of the UE with a new jet area/median approach is in progress. The goal is to produce corrected data for all center of mass and to test the UE modeling is universal: for example using Z bosons.

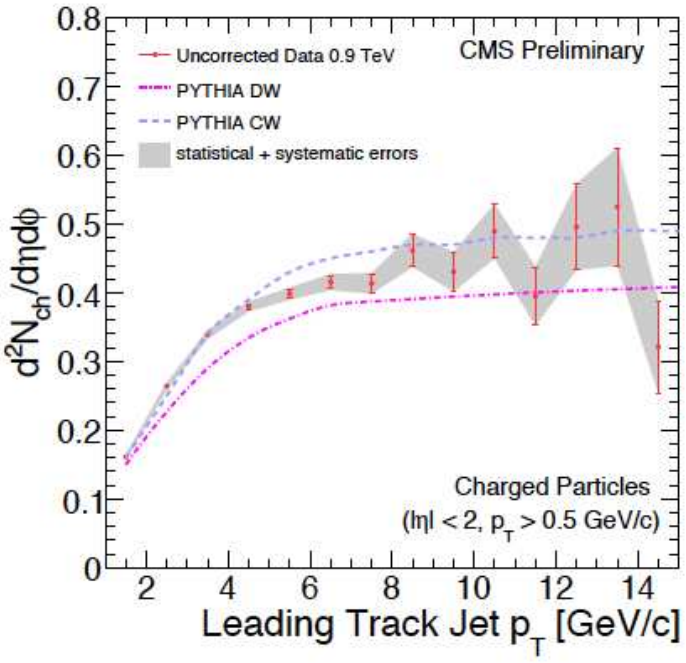

Figure 8: Average multiplicity per unit of pseudorapidity and per radian as a function of the scale provided by the pT of the leading track jet for charged particles in the transverse region, with $pT > 0.5$ GeV/c and $|\eta| < 2$. The error bars indicate the systematic error; the shaded bands correspond to the total experimental error (statistical and systematic errors added in quadrature). Predictions of the CW and DW PYTHIA MC tunes are compared to the uncorrected data.

4.4 Two-Particle Angular Correlations and Cluster Properties in pp Collisions at $\sqrt{s} = 0.9$, 2.36 and 7 TeV

Inclusive two particle correlation [6] was observed in PHOBOS [13] and UA5 [14] and exhibit an approximate Gaussian shape in the relative pseudo rapidity of between any two track with a range of $\sigma_{\Delta\eta} \approx 1$unit. Thus, these correlations have been conventionally described as "short-range". In the case of inclusive correlations, a useful ansatz is to assume that the initial interactions emit so-called "clusters". These clusters are assumed to be emitted independently (ICM) and then to subsequently decay isotropically in their own rest frame into the observed hadrons. Heavier clusters, which would emit more particles, correspond to stronger correla-

tions. This simple cluster description can, therefore, be used to quantitatively characterize this important aspect of particle production for a variety of systems and energies [15]. The observed correlation strength and extent in relative pseudorapidity between the particles are parameterized by a Gaussian distribution. The fitted parameters are the cluster multiplicity, or "size" (the average number of particles into which a cluster decays) and the decay "width" (the separation of the emitted particles in pseudorapidity). In order to measure , the pT-inclusive charged two-particle correlation function in two-particle ($\Delta\eta$,$\Delta\phi$) space, the following quantity was defined in Eq. 1.

$$R(\Delta\eta, \Delta\phi) = \left\langle (N-1)\left(\frac{S_N(\Delta\eta, \Delta\phi)}{B_N(\Delta\eta, \Delta\phi)} - 1\right)\right\rangle_N \quad (1)$$

where N represents the total track multiplicity of each event. The sample was divided into 10 bins in track multiplicity (N), each containing about 10% of all the events. At a fixed multiplicity bin, the signal distribution is the charged two-particle pair density function (normalized to unit integral). It is determined by taking particle pairs within the same event, then averaging over all events. The background distribution denotes the distribution of uncorrelated particle pairs (normalized to unit integral). It is constructed by randomly selecting two different events from the same multiplicity bin and pairing every particle from one event with the other event, representing a product of two single particle distributions. The ratio of the signal to background distribution was first calculated in each multiplicity bin. In this way, all the detector inefficiencies (e.g. tracking, non-uniform acceptance) were canceled. It is then weighted by the track multiplicity factor, $N-1$ (average multiplicity in each bin), and averaged over all the multiplicity bins to arrive at the final two-particle correlation function $R(\Delta\eta, \Delta\phi)$ 1.

$R(\Delta\eta, \Delta\phi)$ at different center of mass energy exhibit the following features: Gaussian-like shape in $\Delta\eta$ and broader at larger $\Delta\phi$. In addition, the near-side peak (small $\Delta\eta$ and $\Delta\phi$) seems enhanced at higher energy. To quantify the clustering properties with data the 2D RN distribution is projected onto relative pseudorapidity plane allowing to measure the size and with of the cluster. The results for the different center of mass energy collision data show that on average, every 2-3 charged particles are produced in a correlated fashion like a cluster. We also find the size of the cluster increasing due to higher p_T objects in the event while the width of the cluster is independent of the center of mass energy. Pythia describes well the trend as a function of the center of mass energy but under estimate the size of the cluster. It could be since Pythia does not describe well the contamination from diffraction events. Last we found by separating the near and away-side correlations that the size of the cluster increase only in the near side. This can be understood in the context of hard and soft processes in QCD. With increasing collision energy contributions from the the hard process are expected to increase and will primarily contribute to the near side where the objects are boosted.

4.5 Measurement of Bose-Einstein correlations in 0.9 and 2.36 TeV proton-proton Collisions with the CMS Experiment

Space time structure of particle emission can be studied via measurements of Bose-Einstein correlations (BEC) between identical bosons. BEC effects are made manifest by the enhanced emission of boson pairs with small relative momenta. Fourier transform of the emission region is essentially the only way to measure the size of a source at the Fermi scale. First observation of BEC occurred fifty years ago in proton-antiproton interactions [16], a number of measurements

have been produced by several experiments using different initial states [17]-[26]. Theoretically, we need to study the ratio between the joint probability of emission of a pair of bosons, and the individual probabilities. Experimentally, we have to produce the distributions of a "proximity" quantity in the data and in a reference sample (Coulomb corrected). To measure the proximity between 2 particles, we chose the difference of their 4-momentum (assuming all pions). To calculate the ratio $R = \frac{dN/dQ}{dN/dQ_{ref}}$ one should take all (charged) tracks to construct a quantity Q and repeat its calculation for the reference sample. Evidence for the effect can be seen in Fig. 9 , where we find the ratios R of the distributions of the invariant mass Q for same-charge particles and a reference sample with the same charge pairs, where one of the two particles has its three-momentum inverted (opposite hemispheres). The ratios for the MC samples with

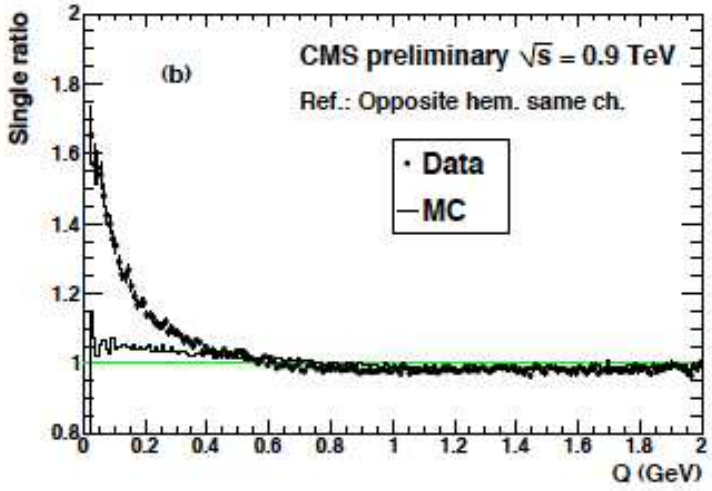

Figure 9: Ratios R of the distributions of the invariant mass Q for same-charge particles and a reference samples of same charge pairs, where one of the two particles has its three-momentum inverted (opposite hemispheres). The ratios for the MC samples with no BEC effect simulated are also shown. Lines at R = 1 are also shown in both figures.

no BEC effect simulated are also shown. To reduce the bias due to the construction of the reference samples, a double ratio $\mathcal{R}$ was defined as in Eq. 2

$$\mathcal{R} = R/R_{\mathrm{MC}} = \left(\frac{\mathrm{d}N/\mathrm{d}Q}{\mathrm{d}N/\mathrm{d}Q_{\mathrm{ref}}}\right) / \left(\frac{\mathrm{d}N/\mathrm{d}Q_{\mathrm{MC}}}{\mathrm{d}N/\mathrm{d}Q_{\mathrm{MC,ref}}}\right), \tag{2}$$

where Q_{MC} and $Q_{\mathrm{MC,ref}}$ refer to the Q distributions from the default simulation, which does not include a modeling of Bose–Einstein correlations. To perform the fit of the double-ratio spectra, the following parameterization given in Eq. 3 of R was used .

$$R(Q) = C\,[1 + \lambda\Omega(Qr)] \cdot (1 + \delta Q). \tag{3}$$

Where λ measures the strength of BEC for incoherent boson emission from independent sources, δ accounts for long-distance correlations, and C is a normalization factor. In a static

model of particle emission, the $\Omega(Qr)$ function is the Fourier transform of the emission region, whose effective size is measured by r. We found phenomenological parameterizations with an exponential shape fit the data significantly better than with a Gaussian shape. One of the subtlety is that an ideal control sample can not be constructed since we could not simply make a sample with a perfect description of the Q distribution in the absence of BEC. Therefore 7 reference samples were constructed however since none of them can be preferred or discarded a priori. Hence a systematic uncertainty is computed as the r.m.s. spread between the results obtained using the different reference samples, i.e. $\pm 7\%$ for λ and $\pm 12\%$ for r. The uncertainty related to the Coulomb corrections was determined with the opposite-charge sample, the predicted strength of the Coulomb effect being compatible with the data within $\pm 15\%$. The corresponding changes are 0.8% for r and 2.8% for λ, which are used as systematic errors. Using the combined reference sample the BEC parameters are thus measured as: $r = 1.59 \pm 0.05$(stat.) ± 0.19 (syst.) fm and $\lambda = 0.625 \pm 0.021$(stat.)$\pm 0.046$ (syst.), for 0.9 TeV data; $r = 1.99 \pm 0.18$ (stat.) ± 0.24 (syst.) fm and $\lambda = 0.663 \pm 0.073$ (stat.)± 0.048(syst.), for 2.36 TeV data. Last but not least, an increase of the parameter r with charged-particle multiplicity in the event is observed.

5 Conclusions

The CMS collaboration completed at the time of the talk its first 5 physics measurements [3]-[7] based on proton-proton collisions delivered by the LHC during 2009 and 2010 at 0.9TeV, 2.36TeV and 7TeV center of mass energy. These measurements helped shed light on on the understanding of the single particle properties and the correlation between the single particles that is essential to understand the mechanism for hadron production and the inelastic process at the highest collision energy. The performance of the detector at start-up was outstanding in particular the excellent performance of the CMS tracker essential for the first CMS measurement was demonstrated. Various other physics analyses are in progress. In addition, a preview of the up coming plans once few p$b^{-1}$of data is recorded reveal promising prospects from the CMS physics analysis groups. In particular, the B-physics finds it feasible to measure Jpsi and Upsilon di-muon decay production cross section differential in p_T and possibly in rapidity. The electroweak analysis group finds it feasible to measure the W and Z cross sections and the cross section ratio of W^+/W^- and W/Z. The first CMS results indicate that CMS can produce high quality physics measurements quickly and new exciting results will be available once more collision data is recorded at 7 TeV.

6 Acknowledgments

I would like to thank the organizers for a very pleasant conference for the many interesting talks stimulating discussions. I thank my CMS colleagues for preparing the results presented in this report,and in particular G. Tonelli, G. Rolandi, D. Acosta, A. De Roeck, R. Tenchini, B. Klima, M. Arneodo, K. Burkett, R. Field, H. Jung, W. Li, M. Mulders, K. Rabbertz and G. Veres for their helpful discussions and suggestions while preparing the talk. On behalf of CMS I also wish to congratulate our colleagues in the CERN accelerator departments for the excellent performance of the LHC machine, thank the technical and administrative staff at CERN and other CMS institutes, and acknowledge support from: FMSR (Austria); FNRS and FWO (Belgium); CNPq, CAPES, FAPERJ, and FAPESP (Brazil); MES (Bulgaria); CERN;CAS, MoST,

and NSFC (China); COLCIENCIAS (Colombia); MSES (Croatia); RPF (Cyprus);Academy of Sciences and NICPB (Estonia); Academy of Finland, ME, and HIP (Finland); CEAand CNRS/IN2P3 (France); BMBF, DFG, and HGF (Germany); GSRT (Greece); OTKA and NKTH (Hungary); DAE and DST (India); IPM (Iran); SFI (Ireland); INFN (Italy); NRF andWCU (Korea); LAS (Lithuania); CINVESTAV, CONACYT, SEP, and UASLP-FAI (Mexico);PAEC (Pakistan); SCSR (Poland); FCT (Portugal); JINR (Armenia, Belarus, Georgia, Ukraine,Uzbekistan); MST and MAE (Russia); MSTDS (Serbia); MICINN and CPAN (Spain); SwissFunding Agencies (Switzerland); NSC (Taipei); TUBITAK and TAEK (Turkey); STFC (UnitedKingdom); DOE and NSF (USA).

References

[1] The CMS Collaboration, CMS Physics Analysis Summary, TRK-10-001 (2010).

[2] The CMS Collaboration, CMS Physics Analysis Summary, QCD-09-010 (2010). JHEP 02 (2010) 041

[3] The CMS Collaboration, CMS Physics Analysis Summary, QCD-10-006 (2010). Phys.Rev.Lett. 105.022002

[4] The CMS Collaboration, CMS Physics Analysis Summary, FWD-10-001 (2010).

[5] The CMS Collaboration, CMS Physics Analysis Summary, QCD-10-001 (2010).

[6] The CMS Collaboration, CMS Physics Analysis Summary, QCD-10-002 (2010).

[7] The CMS Collaboration, CMS Physics Analysis Summary, QCD-10-003 (2010).

[8] The CMS Collaboration, CMS Physics Analysis Summary, MUO-10-00 (2010). Phys.Lett.B692:83-104,2010

[9] K. Aamodt et al.,"Charged-particle multiplicity measurement in proton-proton collisions at sqrt(s) = 0.9 and 2.36 TeV with ALICE at LHC", Eur.Phys.J.C68:89-108,2010

[10] UA5 Collaboration,"Scaling of pseudorapidity distributions at c.m. energies up", Z. Phys. C33 (1986) 1.

[11] V. Barone and E. Predazzi, High-energy particle diffraction, Springer, 2002

[12] O. S. Bruning, P. Collier, P. Lebrun et al.,"LHC Design Report" CERN, Geneva, 2004

[13] PHOBOS:Phys. Rev. C75, 054913 (2007),Phys. Rev. C81, 024904 (2010) (heavy ion)

[14] UA5: Phys.Lett.B123:361,1983

[15] UA5 Collaboration,"CHARGED PARTICLE CORRELATIONS IN ANTI-P P COLLISIONS AT C.M. ENERGIES OF 200-GEV, 546-GEV AND 900-GEV"Z. Phys. C37 1988

[16] G. Goldhaber et al., Phys. Rev. 120 (1960) 300.

[17] MARKII Collaboration, Phys. Rev. D39 (1989) 1.

[18] TASSO Collaboration, Z. Phys. C30 (1986) 355.

[19] Collaboration, Eur. Phys. J. C36 (2004) 147.

[20] DELPHI Collaboration, Phys. Lett. B286 (1992) 201.

[21] L3 Collaboration, Phys. Lett. B524 (2002) 55.

[22] OPAL Collaboration, Phys. Lett. B559 (2003) 131.

[23] UA1 Collaboration, Phys. Lett. B226 (1989) 410.

[24] NA27 Collaboration, Z. Phys. C54 (1992) 21.

[25] NA22 Collaboration, Z. Phys. C37 (1988) 347.

[26] ZEUS Collaboration, Acta Phys. Polon. B33 (2002) 3281